ELSEVIER

Biochimica et Biophysica Acta 1420 (1999) 168–178

BIOCHIMICA ET BIOPHYSICA ACTA
BBA

www.elsevier.com/locate/bba

Kinetic and equilibrium studies of incorporation of di-sulfonated aluminum phthalocyanine into unilamellar vesicles

Nathalie Maman [a], Suman Dhami [b,1], David Phillips [b], Daniel Brault [a,*]

[a] *Laboratoires de Photobiologie et de Biophysique, CNRS UMR 8646, INSERM U. 201, Muséum National d'Histoire Naturelle, 43 rue Cuvier, 75005 Paris, France*

[b] *Department of Chemistry, Imperial College of Science, Technology and Medicine, Exhibition Road, South Kensington, London SW7 2AY, UK*

Received 18 March 1999; received in revised form 17 May 1999; accepted 2 June 1999

Abstract

The interactions of *cis*-di-sulfonated aluminum phthalocyanine (PcS_2Al) with dimyristoylphosphatidylcholine (DMPC) unilamellar vesicles have been investigated by fluorescence spectroscopy. At pH 7.0, PcS_2Al incorporates into the vesicles with a high affinity constant (2.7×10^6 M^{-1}, in terms of phospholipid concentration). The fluorescence changes following rapid mixing of PcS_2Al with vesicles are biphasic. The first phase is attributed to the entry of PcS_2Al into the vesicles, as deduced from the linear dependence of the rate upon lipid concentration. More surprisingly, this rate is strongly pH dependent with a marked maximum around pH 7.3, a result interpreted in terms of the coordination state of the aluminum ion in aqueous solutions. At this pH, a hydroxide ion neutralizes the residual positive charge of the metal ion that remains unbalanced after coordination by the phthalocyanine cycle. A water molecule is likely to complete the metal coordination sphere. Only this form, $PcAl^+(OH^-)(OH_2)$, with an uncharged core is quickly incorporated into the vesicles. The protonation of OH^- or the deprotonation of the coordinated H_2O leading to a positively or negatively charged core, respectively, account for the observed pH effect. Studies on the effect of cholesterol addition and exchange of PcS_2Al between vesicles and albumin all indicate the absence of transfer of the phthalocyanine between the vesicle hemileaflets, a result expected from the presence of the two negatively charged sulfonated groups at the ring periphery. Instead, the slower kinetic phase is likely due to the movement of the phthalocyanine becoming more buried within the outer leaflet upon the loss of the water molecule coordinated to the aluminum ion.

Keywords: Di-sulfonated aluminum phthalocyanine; Lipidic vesicle; Kinetics; Metal coordination; pH; Photodynamic therapy

1. Introduction

Photosensitization is a process that leads a non-toxic molecule (photosensitizer) to produce short-lived reactive species, such as singlet oxygen or free radicals, under light excitation [1]. Owing to their brief lifetime, these active species diffuse less than 0.1 μm in a biological environment [2]. Consequently, they can damage biomolecules only in the vicinity of the photosensitizer. Benefit is derived from this specificity in photodynamic therapy of tumors (PDT) that retain photosensitizers to some extent [3,4]. Porphyrins were among the first photosensi-

* Corresponding author. Fax: +33-1-4079-3705; E-mail: brault@mnhn.fr

[1] Present address: Proctor and Gamble, Rusham Park, Egham, Surrey TW20 9NW, UK.

0005-2736/99/$ – see front matter
PII: S0005-2736(99)00093-0

tizers developed for PDT and approval for a porphyrin based drug, Photofrin, has been recently obtained in various countries. Porphyrin spectral properties are not optimal for PDT, however. In fact, their absorption spectra are not different enough from that of hemoglobin which thus acts as a screen impeding light penetration. Consequently, second-generation photosensitizers with strong absorption bands shifted towards the red have been developed, which makes possible to use excitation light better transmitted by tissues [5]. Phthalocyanines belong to an important class of these new photosensitizers [6].

The efficiency of photosensitizers to inactivate cells is generally correlated with their hydrophobicity and membranes are considered as main targets [7]. The subcellular localization is also a determinant of cell death. Therefore, it is important to characterize more precisely the interactions of photosensitizers with bilayer structures, both with respect to their overall affinity and from a dynamic point of view.

In order to shed light on these processes, interactions of dicarboxylic porphyrins related to Photofrin with membranes have been investigated using unilamellar lipidic vesicles (liposomes) of dimyristoyl- (DMPC) or monounsaturated-phosphatidylcholine as models [8–10]. The existence of two pools of porphyrin molecules located either in the inner or the outer vesicle hemileaflet was demonstrated. The porphyrin was oriented with its core in the hydrophobic phase of the vesicle and its carboxylic chains at the water/phospholipid interface. The entry of the porphyrin in the phospholipidic bilayer, its exit from the outer layer and its movement through the bilayer (flip-flop) were characterized kinetically. The exit and flip-flop rates were found to strongly depend on pH, an effect consistent with the modulation of the ionization state of the side carboxylic chains of the porphyrin [9,10].

In the present study, we focus on the properties of a second generation amphiphilic photosensitizer, *cis*-di-sulfonated aluminum phthalocyanine that shows promising photobiological activity [11–14]. This photosensitizer was found to localize mainly in lysosomes [15,16]. Its two sulfonate side chains remain ionized in the whole pH range of biological interest. Nevertheless, the interactions of this compound with DMPC unilamellar vesicles are found to depend on pH. This unexpected effect is interpreted in terms of a pH-dependent coordination state of the central aluminum ion. The question of the transport of this molecule within cells is also discussed.

2. Materials and methods

2.1. Materials

The dimyristoylphosphatidylcholine (DMPC) and lipid-free human serum albumin (HSA) were purchased from Sigma. The cholesterol was obtained from Aldrich. Di-sulfonated aluminum phthalocyanine was prepared and characterized as described elsewhere [12,17]. The *cis*-isomer, which is the α,α-di-substituted regioisomer with the sulfonate groups on adjacent isoindole units, was isolated using reverse phase HPLC. Its structure is shown in Fig. 1.

2.2. Sample preparation

The experiments were performed using 0.15 M NaCl solutions buffered to different pH values (6–9.5) with phosphate (20 mM) or borate (20 mM). PcS_2Al was readily soluble in these solutions. Small unilamellar vesicles were prepared by extrusion [18,19]. DMPC or DMPC:cholesterol mixtures were dissolved in chloroform or chloroform:methanol (9:1) mixtures. The solutions were taken to dryness and then the lipids were dispersed in buffer by vortexing. The resulting multilamellar liposome suspensions were extruded 8–10 times through a stack of 50 nm polycarbonate filters (Poretics, Livermore, CA) using an extruder device (Lipex Biomembranes, Vancouver, Canada) thermostated at 32°C. The diameter of the vesicles thus prepared was previously determined to be 63 nm, corresponding to about 30 000 phospholipid molecules [8]. In the case of the mixed lipid:cholesterol systems, the solutions were first extruded through 200 nm pores. In experiments involving PcS_2Al preloaded vesicles, the phthalocyanine was introduced in the chloroform mixtures before they were taken to dryness.

2.3. Measurements

Steady-state emission and excitation spectra were

recorded on a Spex spectrofluorometer (Edison, NJ). Kinetic measurements were performed with the aid of a stopped-flow apparatus (Applied Photophysics, Leatherhead, UK) with a mixing time of 1.3 ms. The excitation light provided by a 150-W Xenon short-arc lamp was passed through a monochromator set at 375 nm. The fluorescence of the solution was collected above 645 nm using a low-cut filter (Oriel 51325, Stratford, CT) removing the scattered light. The signal was fed to a RISC workstation (Acorn Computers, Cambridge, UK). It was analyzed by mono-, bi- or tri-exponential fitting curves using the Applied Photophysics software based on a Marquardt non-linear regression algorithm. In preliminary experiments, a Durrum–Gibson stopped-flow apparatus (Palo Alto, CA) with a mixing time of 3 ms was also used. In this case, the fluorescence was collected above 610 nm and kinetics analyzed using home made software.

3. Results

3.1. Steady-state measurements

Initially, the partition of phthalocyanine between the vesicle lipidic phase and the aqueous phase was determined at equilibrium by steady-state fluorescence measurements. The greatest difference between PcS_2Al excitation spectra in pure buffer and in a preformed vesicle solution occurred at around 375 nm, which was subsequently used as the excitation wavelength for emission spectra.

The effect of increasing DMPC vesicles concentration on phthalocyanine emission spectra, at pH 7, is shown in Fig. 2a. The fluorescence maximum shifts upon addition of vesicles from 677 nm in pure buffer to 674 nm, suggesting movement of phthalocyanine from an aqueous to a lipidic environment. The fluorescence intensity also increases while increasing lipid concentration as shown in Fig. 2b. These fluorescence changes were used to determine the affinity constant for incorporation of phthalocyanine into the vesicles, K_{ss}, as described elsewhere [20]. This affinity constant, expressed in terms of the phospholipid concentration, was found to be $(2.7 \pm 0.4) \times 10^6$ M^{-1} at pH 7.

No evidence for dimerization/aggregation was found from the absorption spectra of aqueous solutions of the phthalocyanine at any pH or concentration used in this work. The possibility of phthalocyanine self-association when incorporated within the vesicles was further investigated by looking at the fluorescence maximum with increasing PcS_2Al concentration. In this experiment, the vesicle concentration was kept constant, but high enough (5×10^{-5} M) to allow full incorporation of the phthalocyanine. The results displayed in Fig. 3 show a linear dependence until the PcS_2Al concentration reaches about 2×10^{-7} M. At higher concentrations, divergence from linearity is seen, suggesting PcS_2Al fluorescence self-quenching [21]. Thus, provided that the ratio between the phthalocyanine and the phospholipid concentration does not exceed 0.4%, the phthalocyanine behaves as a monomer and can be considered as fully diluted in the lipidic environment. These conditions prevailed in all of our experiments.

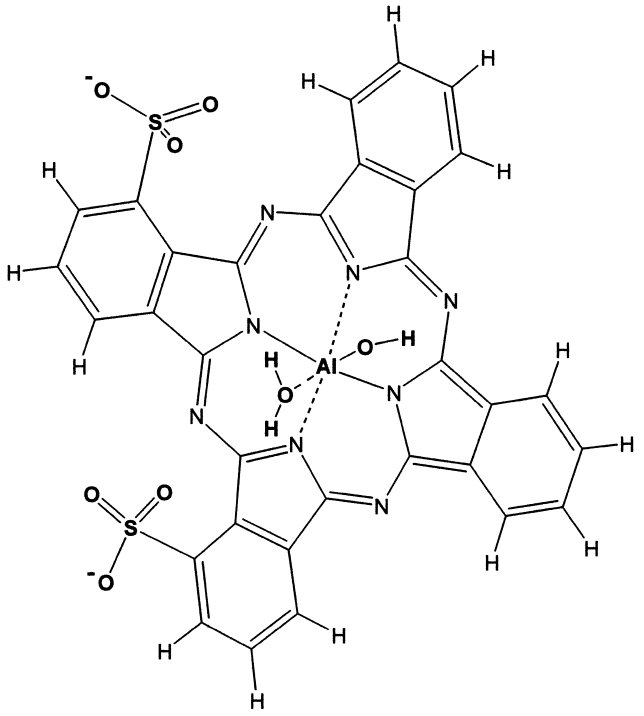

Fig. 1. Structure of *cis*-di-sulfonated aluminum phthalocyanine (PcS_2Al) coordinated by a hydroxide anion and a water molecule.

3.2. Kinetics of incorporation of PcS_2Al into DMPC vesicles

The spectral changes observed in steady-state ex-

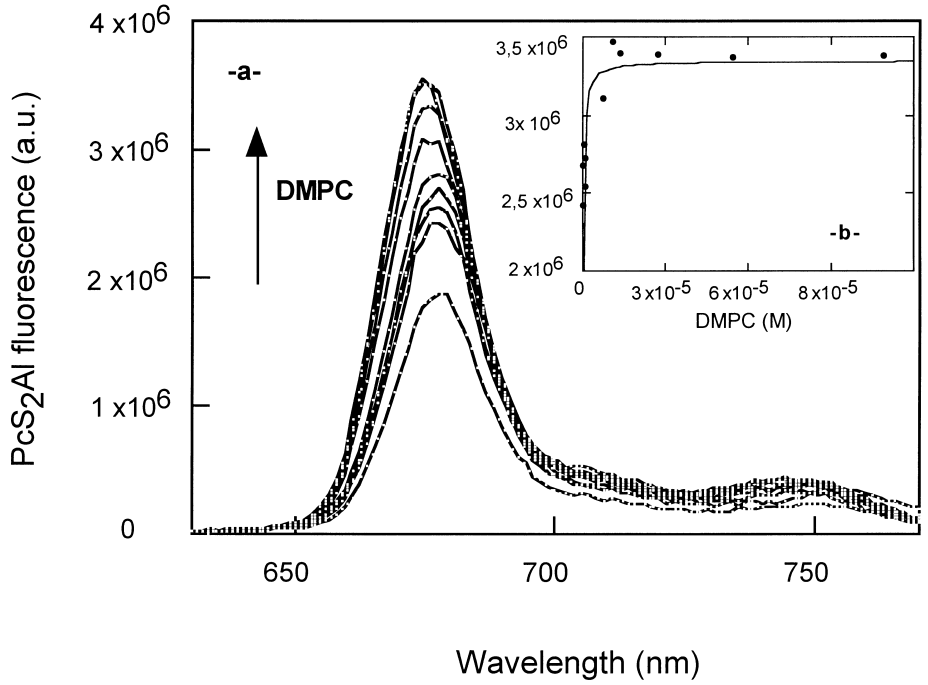

Fig. 2. (a) Emission spectra of PcS_2Al (1×10^{-8} M) in buffer (pH 7.0) and in the presence of various DMPC vesicle concentrations. The excitation wavelength was set at 375 nm. (b) Corresponding changes in the fluorescence intensity at 677 nm. The curve fit is derived from Eq. A5 with $F_o = 1.9\times10^6$ a.u., $F_\infty = 3.5\times10^6$ a.u. and $K_{ss} = 2.70\times10^6$ M^{-1} (phospholipid concentration).

periments were further studied from a kinetic point of view. Phthalocyanine and DMPC vesicles were mixed in the stopped-flow apparatus, with excitation wavelength set at 375 nm. As shown in Fig. 4, the resulting fluorescence signal typically consisted of two phases that can be fitted in most cases by a biexponential function. The phthalocyanine concentration was kept at 1×10^{-7} M in all experiments, whereas DMPC liposomes concentration varied from 5×10^{-5} to 5×10^{-4} M.

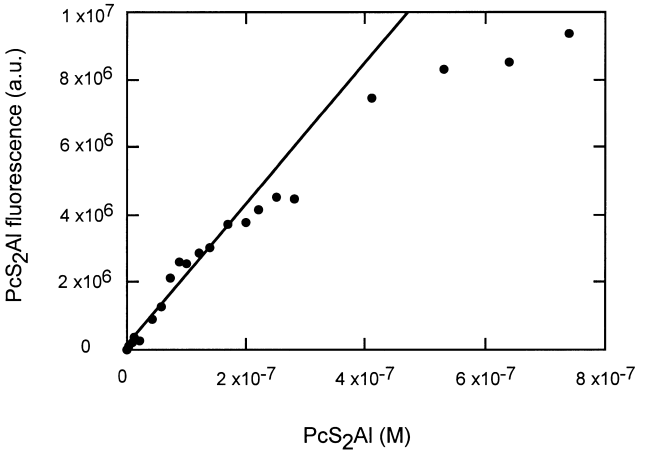

Fig. 3. Dependence of the fluorescence at 677 nm of PcS_2Al incorporated in DMPC vesicles upon concentration. The DMPC concentration was fixed at 5×10^{-5} M and the excitation wavelength at 375 nm. The solution was buffered to pH 7.0.

The incorporation of PcS_2Al into liposomes was studied at different pHs. Phosphate buffer and borate buffer were used from 6.0 to 8.0 and from 8.0 to 9.5, respectively. The nature of the buffer had no effect on the kinetics as checked at pH 8, a value consistent with the buffer range of the two salts. On Fig. 5a and b are presented, for selected pH values, the effect of the lipid concentration on the rate constants of the fast phase, k_1, and the slow phase, k_2, respectively. The rate constant k_1 is linearly dependent on the vesicle concentration, as would be predicted by a simple incorporation theory (see Appendix). In principle, the rate constants for the entry of PcS_2Al into the vesicles can be derived from the slope of such plots. A drastic effect of pH on these slopes is observed, however. As shown in Fig. 6, their values increase while rising pH until about 7.3 and then decrease at higher pH values. The slower rate constant k_2, which might represent a deeper penetration

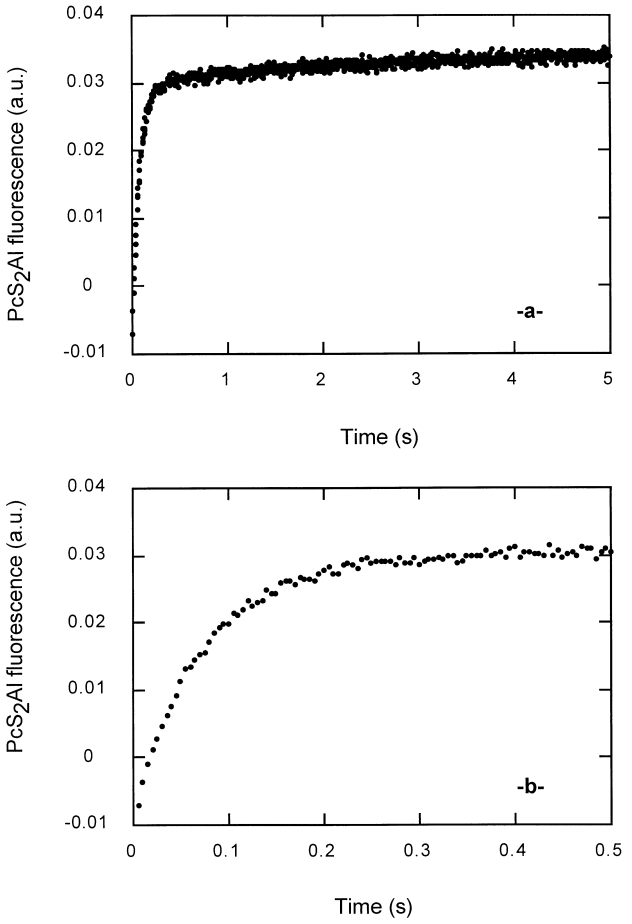

Fig. 4. Change in fluorescence intensity versus time recorded upon mixing DMPC vesicles (2×10^{-4} M) with 1×10^{-7} M $AlPcS_2$ at 32°C, pH 6.3, excitation wavelength set at 375 nm. The slow and fast components are shown in parts a and b, respectively.

of PcS_2Al into the lipid bilayer (see Section 4), is maximum for pH 8.0. The contribution of the slower phase to the total signal is only about one tenth, which results in more erratic rate constant values, however.

Between pH 8.0 and 9.3, a very fast component was observed within less than a few tens of milliseconds after mixing. The amplitude of this transient that preceded the above-mentioned phases was small, however. This third component was not observed outside this pH range.

In order to get insight into the effect of bilayer properties on the kinetics, some experiments were also carried out with DMPC vesicles containing 40% mol/mol of cholesterol. The effect of vesicle concentration on k_1 at pH 7 is shown in Fig. 7. Again, a linear correlation is observed, but the slope, 1.70×10^4 s^{-1} (calculated with respect to the total phospholipid+cholesterol concentration), is significantly lower than that found without cholesterol (8.4×10^4 s^{-1}). The slower rate constant, k_2, did not vary significantly from that obtained with the 'DMPC-only' system.

The possibility of PcS_2Al movement between the two hemileaflets of the bilayer vesicle was checked by investigating its transfer to albumin according to a procedure previously described for dicarboxylic porphyrins [8]. In this case, PcS_2Al was added to the

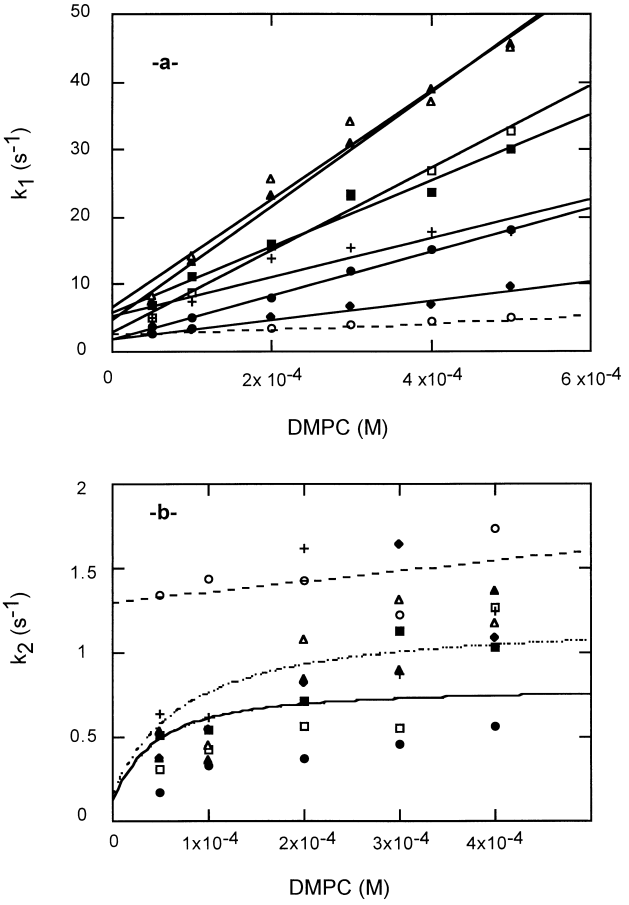

Fig. 5. Plot of the fast (a) and slow (b) phase rate constants, k_1 and k_2 versus DMPC concentration for pH (●) 6.0, (□) 6.5, (▲) 7.0, (△) 7.5, (■) 8.0, (+) 8.2, (◆) 9.0 and (○) 9.5. The linear fits are given by Eq. A8. The curves, presented in b, correspond to the theoretical fits given by Eq. A6 for pH 6.0 (——) and 7.5 (- · - · -) with $k_{on}^{obs}=3.3\times10^4$ and 8×10^4 M^{-1} s^{-1}, $k_{off}=1.3$ and 5.5 s^{-1}, $k_{in}=0.4$ and 0.9 s^{-1}, $k_{ex}=0.1$ and 0.3 s^{-1}, respectively. The dashed line shows that, at pH 9.5, the concentration of DMPC vesicles had nearly no effect on the two rate constants.

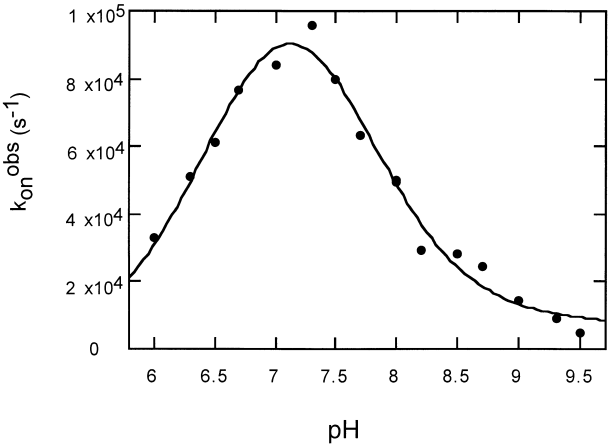

Fig. 6. Changes of the entry rate constant k_{on}^{obs} with pH. The theoretical curve has been fitted using Eq. 1 with $pK_1 = 6.54$, $pK_2 = 7.67$ and $k_{on} = 1.37 \times 10^5$ M^{-1} s^{-1}.

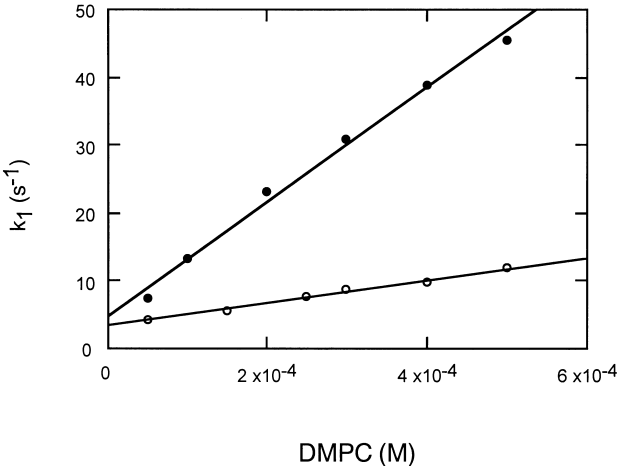

Fig. 7. Dependence of the fast rate constant k_1 on (●) DMPC and (○) DPMC/cholesterol vesicles concentration. The PcS_2Al concentration was fixed at 1×10^{-7} M and the excitation wavelength set at 375 nm.

lipid mixture before vesicle preparation and was expected to partition between the two hemileaflets. An excess of albumin was then added to the vesicle/phthalocyanine mixture and the fluorescence emission spectrum monitored over time. The emission spectra of PcS_2Al+HSA with no vesicles added and the one of PcS_2Al+HSA+vesicles (i.e. PcS_2Al was not preloaded into vesicles, but added subsequently) served as control for full PcS_2Al transfer to albumin. On addition of HSA, an initial fast change in the fluorescence intensity is observed which is followed by a much slower one that extend over hours until eventually all of the phthalocyanine is bound to the

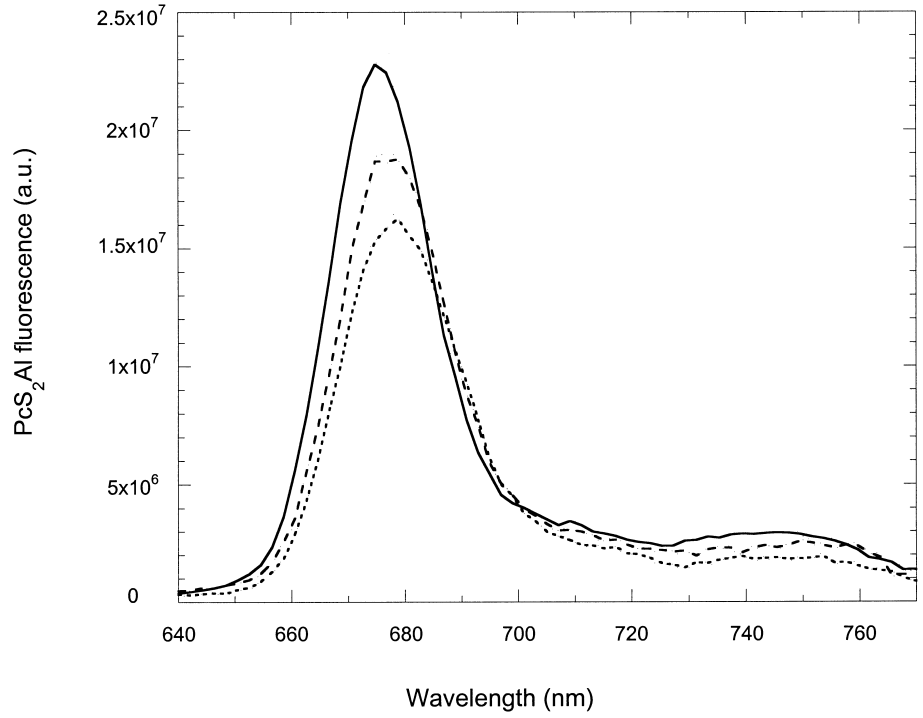

Fig. 8. Transfer of PcS_2Al from vesicles to albumin. Emission spectra of 5×10^{-8} M of PcS_2Al preloaded in DMPC vesicles (——), in DMPC vesicles/albumin mixture just after adding albumin (- - -), added to a mixture of DMPC vesicles and albumin (· · ·).

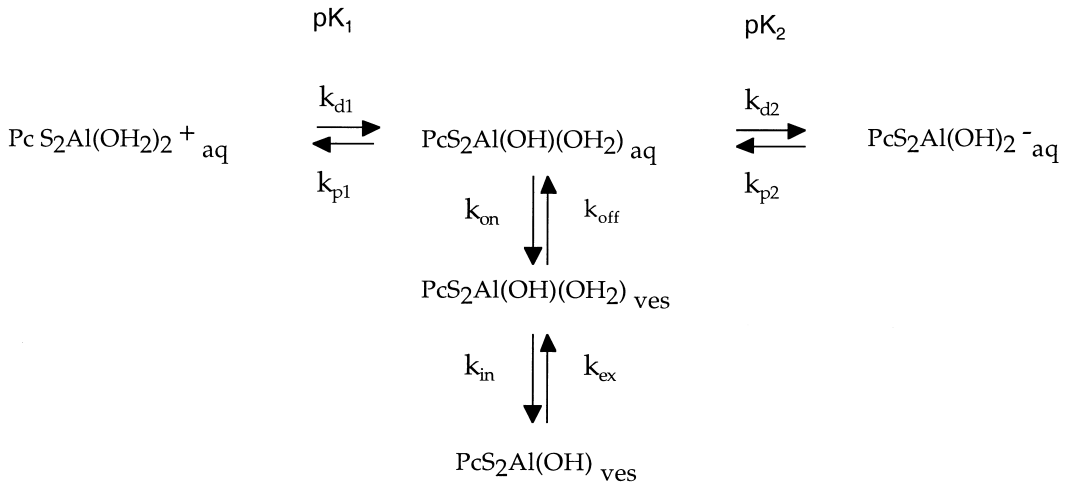

Fig. 9. Scheme for the incorporation of PcS_2Al in vesicles. The upper line shows protonation equilibria taking place at the water interface. The incorporation into the vesicles is shown to proceed in two steps. The second one is expected to correspond to the movement of the phthalocyanine to a deeper location within the bilayer associated with the loss of a water molecule.

HSA as ascertained from the control spectra (see Fig. 8).

4. Discussion

Despite the negative charges of its sulfonate groups, PcS_2Al displays a very high affinity for DMPC vesicles, about one order of magnitude higher than that of deuteroporphyrin, a hydrophobic dicarboxylic porphyrin. It is likely that this higher affinity is provided by the benzyl rings fused to the pyrroles, increasing hydrophobic interactions with the lipidic phase of the bilayer. This observation suggests that the phthalocyanine is located in such a conformation so as to allow the charged sulfonate groups to remain in the outer aqueous phase (where they will be hydrated) whilst the neutral hydrophobic moiety is buried in the lipidic core.

The linear dependence of the fast rate constant, k_1, on DMPC concentration indicates that this step corresponds to the incorporation of the phthalocyanine into the vesicles. The effect of pH on the magnitude of k_1 is more surprising. Indeed, the pK_a of the sulfonate groups is estimated to be less than 1 [22] and so, these groups will always remain ionized in the pH range used in this study. Therefore, any effects of pH are most likely indicative of changes in the ligands associated with the central aluminum. It must be pointed out that a residual positive charge on the aluminum ion remains unbalanced after coordination by the phthalocyanine cycle. Aluminum derivatives of phthalocyanines always crystallize with an associated anion bound to the metal (see Fig. 1). In aqueous solution, the neutrality at the center of the macrocycle is most likely achieved through coordination of aluminum by a hydroxide anion. Binding of a water molecule in a *trans*-position would complete the coordination sphere of aluminum. As shown by Savitsky et al. [23], these ligands can undergo acid-base equilibria according to the top row of the scheme depicted in Fig. 9. The pK values of these equilibria have been determined to be 6.7 and 9.7 in aqueous solutions. The species, $PcAl(OH_2)_2^+$ and $PcAl(OH)_2^-$ that predominate at the lowest and highest pH, respectively, possess an unbalanced charge at the center of the macrocycle, a fact that would hinder penetration within the lipidic phase of the vesicles. In the porphyrin series, protonation of inner nitrogens impedes incorporation into the lipidic bilayer [24]. Therefore, it seems likely that only the $PcAl(OH)(OH_2)$ form incorporates into the vesicles. As detailed in the result section, in most cases, the interactions of the phthalocyanine with vesicles are characterized by a first phase that can be fitted by an exponential yielding a rate constant k_1. This constant linearly depends on the phospholipid concentration in the whole pH range investigated. Pseudo-first order conditions prevail. Regardless of the relative ratio of the $PcAl(OH_2)_2^+$, $PcAl(OH_2)(OH)$ and

$PcAl(OH)_2^-$ species, only one phthalocyanine population can be observed indicating that the incorporation is preceded by a fast acid-base equilibrium leading to the formation of the $PcAl(OH)(OH_2)$ species. This observed pseudo-first order rate constant (the slope of the plot of k_1 versus the lipid concentration) would be a combination of the intrinsic rate constants for each form of the phthalocyanine weighted by its relative abundance. In keeping with the above comments, only the $PcAl(OH_2)(OH)$ form was assumed to incorporate with the rate constant k_{on}. Thus, the observed rate constant, k_{on}^{obs} can be expressed as:

$$k_{on}^{obs} = k_{on} \times 10^{-(pK1+pH)} / \{10^{-2pH} + 10^{-(pK1+pH)} + 10^{-(pK1+pK2)}\} \quad (1)$$

As shown in Fig. 6, the experimental results are quite well fitted by this relation with pK values of 6.54 and 7.67 and a rate constant k_{on} of $(1.37 \pm 0.20) \times 10^5$ M^{-1} s^{-1} expressed in terms of lipid concentration. It might be surprising that these pK values are shifted to such a large extent as compared to those reported for aqueous solutions. However, these values refer to the pH at the phospholipid/water interface which can be quite different from that of the bulk solution.

By using these pK values, it is possible to further check the validity of the assumption that fast protonation equilibria precede the incorporation step. In the acidic range, deprotonation of $PcAl(OH_2)_2^+$ is the prerequisite to incorporation. This reaction rate, k_{d1}, is equal to $k_{p1} \times 10^{-pK1}$, where k_{p1} is the reaction rate constant for $PcAl(OH_2)(OH)$ protonation. As the latter is expected to be diffusion limited [25], i.e. in the range $1–3 \times 10^{10}$ M^{-1} s^{-1}, k_{d1} can be computed to be around $(3–10) \times 10^3$ s^{-1}. Thus, deprotonation of $PcAl(OH_2)_2^+$ is faster than the dead time of our stopped flow apparatus. In the alkaline range, the prerequisite is protonation of $PcAl(OH)_2^-$, a bimolecular step. Assuming again a protonation rate constant around $1–3 \times 10^{10}$ M^{-1} s^{-1}, it appears that, above about pH 8, the time to attain protonation equilibria exceeds milliseconds. Numerical simulations (see Appendix for details) involving all the reaction steps of the scheme shown in Fig. 9 do predict that, in this pH range, a fast component should precede the step characterized by the rate constant k_1, which was experimentally observed. Although the amplitude of this fast component was small, it might be responsible for some overestimation of k_1 and could account for some discrepancy between the theoretical fit and experimental data above pH 8.5 as seen in Fig. 6. At the highest pH value, the protonation of $PcAl(OH)_2^-$ becomes the rate-limiting step and the observed kinetics no more depend on the vesicles concentration as shown in Fig. 5 (dashed line).

The mechanism of the incorporation of the phthalocyanine into the vesicles can be further elucidated by considering the value of the rate constant k_{on} expressed in terms of the vesicle concentration. It can be calculated by multiplying the lipid expressed value by the number of phospholipid molecules in each vesicle (about 30 000). We obtain $k_{on} = 3.9 \times 10^9$ $vesicle^{-1}$ s^{-1}. This value can be compared to that of a diffusion limited step [26]. This limit is given by:

$$k_d = 4\pi(R_v + R_p)(D_v + D_p)N \quad (2)$$

where R_v and R_p are the radius of the vesicle and phthalocyanine, D_v and D_p are the diffusion coefficients of the vesicle and phthalocyanine, respectively. N is the Avogadro number. Compared to the vesicles, the size of the phthalocyanines can be neglected. The diffusion coefficient of phthalocyanines can be estimated from that of porphyrins by taking into account the difference in radius which yields about $1–1.5 \times 10^{-10}$ m^2 s^{-1}. The diffusion coefficient of the vesicles ($< 1 \times 10^{-11}$ m^2 s^{-1}) is much lower. Using this equation, the diffusion limit is estimated to be $\sim 3 \times 10^{10}$ M^{-1} s^{-1}. Thus, the value of k_{on}, 3.9×10^9 $vesicle^{-1}$ s^{-1}, is about one order of magnitude lower than the diffusion limit. It is likely that the incorporation involves some initial activation step, such as modification of the solvation sphere around the aluminum ion, which facilitates interaction of the phthalocyanine with the vesicles. For comparison, the entry of carboxylic porphyrins which does not involve such loss of ion solvation was found to be limited only by diffusion [27].

The slower phase characterized by the rate constant k_2 remains to be assigned. It could be assumed that it corresponds to the 'flip-flop' of the phthalocyanine between the two vesicle hemileaflets. Such a behavior was observed with dicarboxylic porphyrins. Even if the fluorescence properties of the dye in the

two environments are similar, it has been demonstrated that a biphasic signal can be observed in a given vesicle concentration range. Indeed, upon movement of the dye towards the inner leaflet, sites are liberated on the outer leaflet, making possible further dye binding from the aqueous phase. In our case, the 'flip-flop' hypothesis can be ruled out, however. First, the addition of cholesterol to the vesicles produces a decrease in the fast rate constant, as would be expected from a more ordered and rigid vesicle system, but showed little effect on the slower rate constant. Previous studies have shown that in the presence of 40% cholesterol, the flip-flop of porphyrins is almost abolished [8]. The data on the transfer of the phthalocyanine to albumin further confirm that flip-flop is not taking place within the stopped flow time range. In these experiments, PcS_2Al being added to the lipid mixture before vesicle preparation, it is expected to partition between the two hemileaflets. Albumin has been demonstrated [15] to have a good affinity ($\approx 10^5$ M^{-1}) for PcS_2Al. On mixing with the vesicles, only half of the preloaded phthalocyanine is quickly transferred to albumin as shown in Fig. 8. A complete transfer is achieved only after several hours.

It can be concluded that the flip-flop of PcS_2Al is many orders of magnitude slower than the second phase observed in stopped flow experiments. This phase could be due to the movement of the phthalocyanine deeper into the lipidic core of the vesicle, thus resulting in two locations for the fluorophore. This process may be driven by the loss of water coordinated to aluminum.

The overall scheme is depicted in Fig. 9. Theoretical equations expressing the rate constants of the two experimentally observed phases as function of the DMPC concentration and intrinsic rate constants are given in the Appendix. In addition to k_{on} and pK values which can be determined quite accurately as shown above, some estimates can be given for the other rate constants. The extrapolation of the rate constant k_2 to high lipid concentration yields the sum $k_{in}+k_{ex}$. As experimental data are quite scattered, it can be only estimated from Fig. 5b that $k_{in}+k_{ex}$ lies in the range 0.5–1.5 s^{-1}. Theoretical plots using two sets of estimated values are shown in Fig. 5b. The extrapolation to zero of the plots of k_1 as a function of DMPC concentration yields $k_{off}+k_{in}+k_{ex}$. Owing to the uncertainty on the extrapolation and on the $k_{in}+k_{ex}$ value, k_{off} can be roughly estimated to be around 1–6 s^{-1}. The equilibrium constant for occupancy of 'external sites' derived from these rate constants, i.e. k_{on}/k_{off}, would be around 10^5 M^{-1}, i.e. at least one order of magnitude lower than the equilibrium constant obtained in steady-state conditions. As the final equilibrium state, including movement of the phthalocyanine towards inner locations, is achieved in steady-state measurements, this difference indicates that the inner location is favored, i.e. $k_{in} \gg k_{ex}$.

5. Conclusion

On mixing *cis*-di-sulfonated aluminum phthalocyanine with DMPC unilamellar vesicles, two phases are observed in the pH range 6–9.5. The dependence of their kinetics on vesicle concentration, pH and cholesterol addition, as well as control studies involving transfer to albumin make it possible to assign these two phases. The faster rate constant, k_1, is related to the initial incorporation of the phthalocyanine into the vesicles. Only the form with no charge in the center of the macrocycle ($PcS_2Al(OH_2)(OH)$) incorporates, the negative sulfonate groups remaining exposed to the aqueous phase. The slower rate constant is not due to 'flip-flop', i.e. movement of the phthalocyanine from the outer to the inner vesicle hemileaflet, but is assigned to the motion of the phthalocyanine into deeper regions of the lipidic core of the vesicle. Acid base equilibria involving the ligands bound to the aluminum ion are responsible for a remarkable pH effect that finds expression in a marked optimum of the incorporation rate around the physiological pH. However, the transport of the phthalocyanine across the bilayer appears to be very slow, excluding passive diffusion as a main mechanism of intracellular localization. These data correlate with the subcellular localization of di-sulfonated phthalocyanines that are mainly retained in lysosomes [15,16]. Accordingly, endocytosis is likely to be the major pathway of cellular uptake [28]. In contrast, Photofrin which is made of carboxylic porphyrins can enter the cell primarily by diffusion across the membrane [28]. Even if Photofrin is taken up by endocytosis, it will leak out from the lyso-

somes by a diffusion process driven by the pH gradient between the lysosome compartment and the cytoplasm [9] and will relocalize in membrane-rich structures. Actually, Photofrin stains mitochondria [29]. These examples show that the thermodynamic and kinetic parameters characterizing the interactions of photosensitizers with membrane models can provide a rational basis to explain their cellular uptake and subcellular localization. The knowledge of these parameters is likely to greatly help to develop more efficient photosensitizers.

Acknowledgements

This work was supported by Grant 7209 from ARC and a CEE contract ERBCHRXCT930178.

Appendix. Incorporation of PcS_2Al in vesicles: theoretical relations

A.1. Equilibrium studies

The steady-state association constant between DMPC vesicles and PcS_2Al can be expressed as:

$$K_{ss} = [PcS_2Al_{DMPC}]/([DMPC]\times[Pc]) \quad (3)$$

or

$$K_{ss} = (F-F_o)/((F_\infty-F)\times[DMPC])) \quad (4)$$

where F_o and F_∞ are the fluorescence intensities corresponding to no and full incorporation of PcS_2Al in the vesicles, respectively.

It can be derived that:

$$F = F_o + ((K_{ss}\times[DMPC]\times(F_\infty-F_o))/(1 + K_{ss}\times[DMPC])) \quad (5)$$

A.2. Kinetic studies

It is assumed that only the $PcS_2Al(OH)(OH_2)$ form incorporates with a rate constant k_{on}. The incorporation process can be described as:

$$PcS_2Al(OH)(OH_2)_{aq} + DMPC \underset{k_{off}}{\overset{k'_{on}}{\rightleftarrows}} PcS_2Al(OH)(OH_2)_{ves} \underset{k_{ex}}{\overset{k_{in}}{\rightleftarrows}} PcS_2Al(OH)_{ves}$$

where $k'_{on} = k_{on}\times[DMPC]$.

The kinetics corresponding to these equilibria consist in two exponential phases whose rate constants can be expressed as:

$$k_{1,2} = 1/2\times\{\Sigma k \pm ((\Sigma k)^2-4\times(k'_{on}\times(k_{in}+k_{ex})+k_{off}\times k_{ex}))^{1/2}\} \quad (6)$$

where Σk is defined as $k'_{on}+k_{off}+k_{in}+k_{ex}$If $(4\times(k'_{on}\times(k_{in}+k_{ex})+k_{off}\times k_{ex}))/(\Sigma k)^2$ is small compared to 1 (our experimental results give $<1\%$), the square root can be developed as a Taylor series, therefore Eq. A6 can be written as:

$$k_{1,2} = 1/2\times\Sigma k\times[1 \pm (1-(2(k'_{on}\times(k_{in}+k_{ex})+k_{off}\times k_{ex})/(\Sigma k)^2))] \quad (7)$$

Changing k'_{on} in $k_{on}\times[DMPC]$, and neglecting small terms gives:

$$k_1 \cong k_{on}\times[DMPC] + k_{off} + k_{in} + k_{ex} \quad (8)$$

and the extrapolation of k_2 versus [DMPC] gives $k_{in}+k_{ex}$.

Full details on the mathematical derivation of these formula can be found in [8,20].

When we can consider that the protonation/deprotonation equilibria are reached (i.e. in the 6.0–8.0 range), k_{on} is replaced by k_{on}^{obs}, a pH-dependent constant as described in the text.

When the protonation/deprotonation equilibria are not reached (cf. Section 4), the kinetics do not consist of only two exponentials. In this case, numerical simulations were performed using the whole set of the differential equations describing the various steps shown in Fig. 9. The Mathcad software (Mathsoft, UK) was used to this end.

References

[1] J.D. Spikes, Photodynamic reactions in photomedicine, in:

J.D. Regan, J.A. Parrish (Eds.), The Science of Photomedicine, Plenum Press, New York, 1982, pp. 113–144.
[2] J. Moan, K. Berg, Photochem. Photobiol. 53 (1991) 549–553.
[3] T.J. Dougherty, W.R. Potter, D. Bellnier, Photodynamic therapy for the treatment of cancer: current status and advances, in: D. Kessel (Ed.), Photodynamic Therapy of Neoplastic Disease, Vol. 1, CRC Press, Boston, MA, 1990, pp. 1–19.
[4] H.I. Pass, J. Natl. Cancer Inst. 85 (1993) 443–456.
[5] R.W. Boyle, D. Dolphin, Photochem. Photobiol. 64 (1996) 469–485.
[6] J.D. Spikes, Photochem. Photobiol. 43 (1986) 691–699.
[7] K.W. Woodburn, S. Stylli, J.S. Hill, A.H. Kaye, J.A. Reiss, D.R. Phillips, Br. J. Cancer 65 (1992) 321–328.
[8] K. Kuzelova, D. Brault, Biochemistry 33 (1994) 9447–9459.
[9] K. Kuzelova, D. Brault, Biochemistry 34 (1995) 11245–11255.
[10] N. Maman, D. Brault, Biochim. Biophys. Acta 1414 (1998) 31–42.
[11] B. Paquette, H. Ali, R. Langlois, J.E. Van Lier, Photochem. Photobiol. 47 (1988) 215–220.
[12] S.M. Bishop, B.J. Khoo, A.J. MacRobert, M.S.C. Simpson, D. Phillips, A. Beeby, J. Chromatogr. 646 (1993) 345–350.
[13] Q. Peng, J. Moan, Br. J. Cancer 72 (1995) 565–574.
[14] W.S. Chan, N. Brasseur, C. La Madeleine, R. Ouellet, J.E. Van Lier, Eur. J. Cancer 33 (1997) 1855–1859.
[15] M. Ambroz, A.J. MacRobert, J. Morgan, G. Rumbles, M.S.C. Foley, D. Phillips, J. Photochem. Photobiol. B: Biol. 22 (1994) 105–117.
[16] J. Moan, K. Berg, H. Anholt, K. Madslien, Int. J. Cancer 58 (1994) 865–870.
[17] M. Ambroz, A. Beeby, A.J. MacRobert, M.S.C. Simpson, R.K. Svensen, D. Phillips, J. Photochem. Photobiol. B: Biol. 9 (1991) 87–95.
[18] F. Olson, C.A. Hunt, F.C. Szoka, W.J. Vail, D. Papahadjopoulos, Biochim. Biophys. Acta 557 (1979) 9–23.
[19] L.D. Mayer, M.J. Hope, P.R. Cullis, Biochim. Biophys. Acta 858 (1986) 161–168.
[20] D. Brault, C. Vever-Bizet, T. Le Doan, Biochim. Biophys. Acta 857 (1986) 238–250.
[21] S. Dhami, G. Rumbles, A.J. MacRobert, D. Phillips, Photochem. Photobiol. 65 (1997) 85–90.
[22] A. Albert, E.P. Serjeant Ionization Constants of Acids and Bases, Methuen, London, 1962.
[23] A.P. Savitsky, K.V. Lopatin, N.A. Golubeva, M.Y. Poroshina, N.V. Stepanova, L.I. Solovieva, E.A. Lukyanets, J. Photochem. Photobiol. B: Biol. 13 (1992) 327–333.
[24] D. Brault, C. Vever-Bizet, K. Kuzelova, J. Photochem. Photobiol. B: Biol. 20 (1993) 191–195.
[25] M. Eigen, L. De Maeyer, Relaxation methods, in: S.L. Friess, E.S. Lewis, A. Weissberger (Eds.), Part Investigation of Rates and Mechanisms of Reactions, Vol. II, Interscience, New York, 1963, pp. 895–1054.
[26] P.W. Atkins, Physical Chemistry, 4th edn., Oxford University Press, Oxford, 1990.
[27] C. Vever-Bizet, D. Brault, Biochim. Biophys. Acta 1153 (1993) 170–174.
[28] W.G. Roberts, M.W. Berns, Lasers Surg. Med. 9 (1989) 90–101.
[29] B.C. Wilson, M. Olivo, G. Singh, Photochem. Photobiol. 65 (1997) 166–176.